ELECTRONIC SUPPORTING INFORMATION (ESI)

for

A Chromotropic $Pt^{II}Pd^{II}Co^{II}$ Coordination Polymer with Dual Electrocatalytic Activity for Water Reduction and Oxidation

Anna Carissa M. San Esteban, Naoto Kuwamura, Nobuto Yoshinari and Takumi Konno*

Department of Chemistry, Graduate School of Science, Osaka University, Toyonaka, Osaka 560-0043, Japan

E-mail: konno@chem.sci.osaka-u.ac.jp

Table S1. Crystallographic data for [**2**]X_4.

	[**2**]Cl_4	[**2**]Br_4
Formula	$C_{20}H_{92}Cl_4Co_2N_8O_{30}Pd_2Pt_2S_4$	$C_{20}H_{92}Br_4Co_2N_8O_{30}Pd_2Pt_2S_4$
Colour, shape	Orange, platelet	Orange, platelet
M	1915.89	2093.73
Crystal system	Orthorhombic	Orthorhombic
Space group	$P2_12_12_1$	$P2_12_12_1$
a /Å	9.0942(2)	9.25625(5)
b /Å	21.9908(5)	21.99085(11)
c /Å	30.830(8)	30.87849(16)
α /°	90	90
β /°	90	90
γ /°	90	90
V /Å^3	6165.7(16)	6285.40(6)
Z	4	4
T /K	100(2)	100(2)
F(000)	3768	4056
ρ_{calcd} /g cm^{-3}	2.064	2.213
μ /mm^{-1}	6.007	2.491
Crystal size /mm^3	0.16×0.10×0.03	0.08×0.05×0.04
Limiting indices	$-9 \le h \le 11$, $-29 \le k \le 21$, $-38 \le l \le 34$	$-14 \le h \le 13$, $-35 \le k \le 37$, $-45 \le l \le 44$
R_1 ($I>2\sigma(I)$) [a]	0.0410	0.0394
wR_2 (all data) [b]	0.0973	0.1041
GOF	1.042	1.050
Flack parameter	0.015(4)	0.040(5)
CCDC No.	2074818	2074819

[a] $R_1 = \Sigma(|Fo|-|Fc|)|/\Sigma(|Fo|)$. [b] $wR_2 = [\Sigma w(Fo^2-Fc^2)^2/\Sigma w(Fo^2)^2]^{1/2}$.

Table S2. Bond valence sum (BVS) calculations for Co atoms in [**2**]X_4.[S1]

	[**2**]Cl_4		[**2**]Br_4	
	Co^{II}	Co^{III}	Co^{II}	Co^{III}
Co1	2.01	1.77	1.99	1.75
Co2	2.00	1.73	2.01	1.73

Table S3. Best fitted parameters for $\chi_M T$ versus T plots of [**2**]X_4.

	[**2**]Cl_4 (heating)	[**2**]Cl_4 (cooling)	[**2**]Br_4 (heating)	[**2**]Br_4 (cooling)
J / cm^{-1}	–0.966(7)	–0.03(3)	–0.856(7)	–0.12(2)
B^0_2 / cm^{-1}	+108.7(12)	+11.3(5)	+118.3(11)	+13.2(4)
g_{iso}	2.0758(14)	2.322(7)	2.0472(11)	2.306(6)
T.I.P.	–0.00188(6)	0.00075(13)	–0.00130(5)	0.00121(11)
F [a]	2.34×10^{-6}	5.00×10^{-5}	2.56×10^{-6}	2.65×10^{-5}

[a] The agreement factor (F) is defined as $\Sigma[\chi_M T_{exp} - \chi_M T_{calcd}]^2/\Sigma[\chi_M T_{exp}]^2$.

Table S4. Summary of representative heterogeneous water oxidation catalysts based on cobalt(II) coordination compounds.

Compound	Overpotential [a]	TOF	Electrolyte	Reference #
[**2**]Br_4	363 mV	0.0044 s^{-1}	0.1 M $LiClO_4$ in H_2O/CH_3CN (1/4)	This work
$[Mn_2(H_2O)_6(\mathbf{1})]Br_4$	384 mV	0.0025 s^{-1}	0.1 M $LiClO_4$ in H_2O/CH_3CN (1/4)	This work, S2
$[Zn(Cu_2\{Pt(NH_3)_2(D\text{-}pen)_2\}_2)](ClO_4)_2$	-	0.0075 s^{-1}	0.1 M KPF_6 in H_2O/CH_3CN (1/4)	S3
$[Co_2(L)(adip)_2]$ [b]	460 mV	0.00068 s^{-1} [c]	0.2 M Pi buffer (pH 6.8)	S4
$[Co_2(L)_2(5\text{-}bdc)_2(H_2O)_2]$ [b]	570 mV	0.00076 s^{-1} [c]	0.2 M Pi buffer (pH 6.8)	S4
$[\{Co_3(\mu_3\text{-}OH)(BTB)_2(dpe)_2\}\{Co(H_2O)_4(DMF)_2\}_{0.5}]_n$ [b]	390 mV	0.05 s^{-1}	0.1 M KOH aq.	S5

[a] at 1 mA /cm^2. [b] L = 1,4-bis(3-pyridylaminomethyl)benzene, H_2adip = adipic acid, 5-H_2adc = 5-nitroisophthalic acid), H_3BTB=1,3,5-benzenetribenzoic acid, dpe=1,2-di(4-pyridyl)ethylene, dppeO_2 = 1,2-bis(diphenylphosphino)ethane dioxide. [c] We calculated the values based on values provided in the literature.

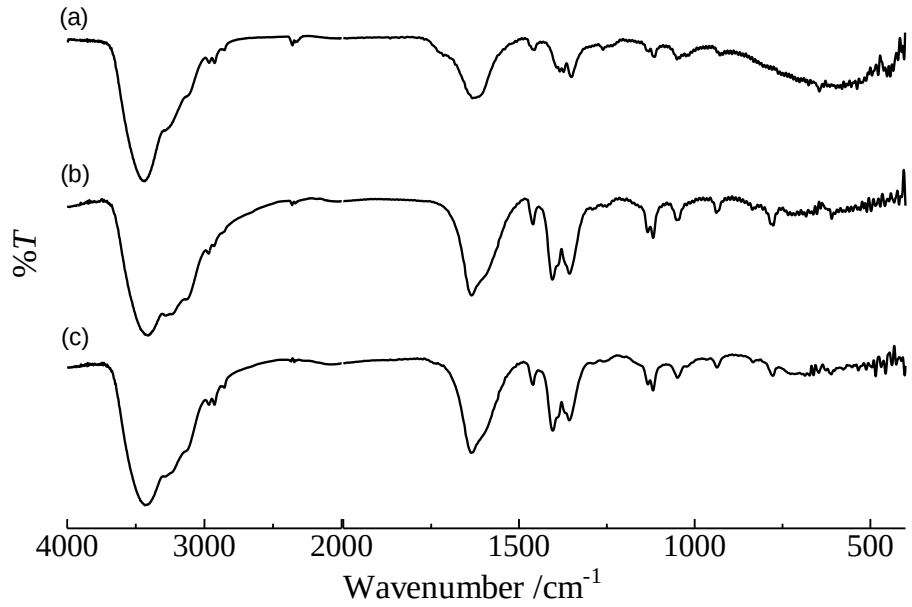

Fig. S1. IR spectra of (a) [**1**], (b) [**2**]Cl_4, and (c) [**2**]Br_4.

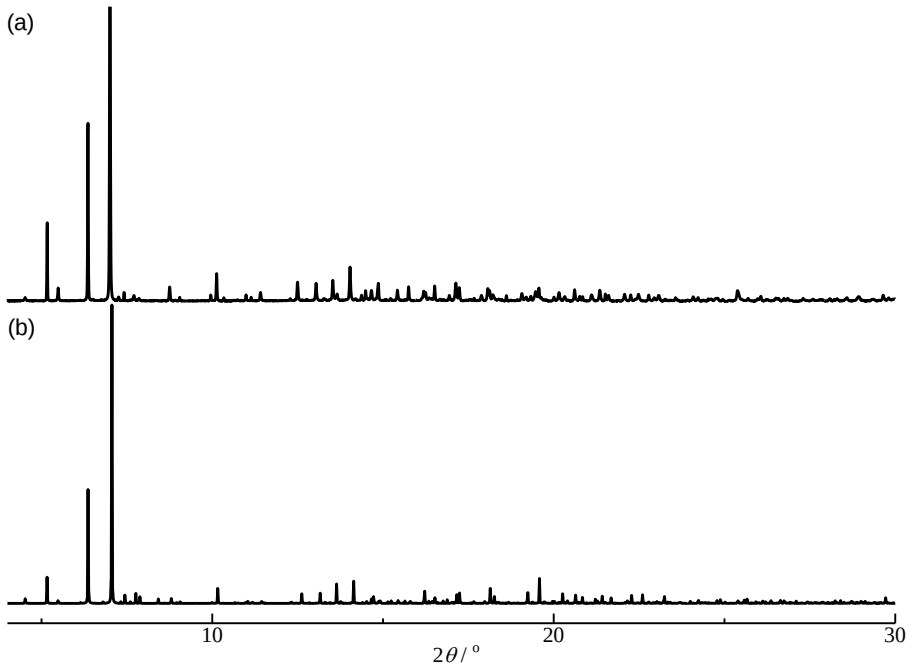

Fig. S2. (a) Experimental and (b) simulated PXRD patterns of [**2**]Cl_4.

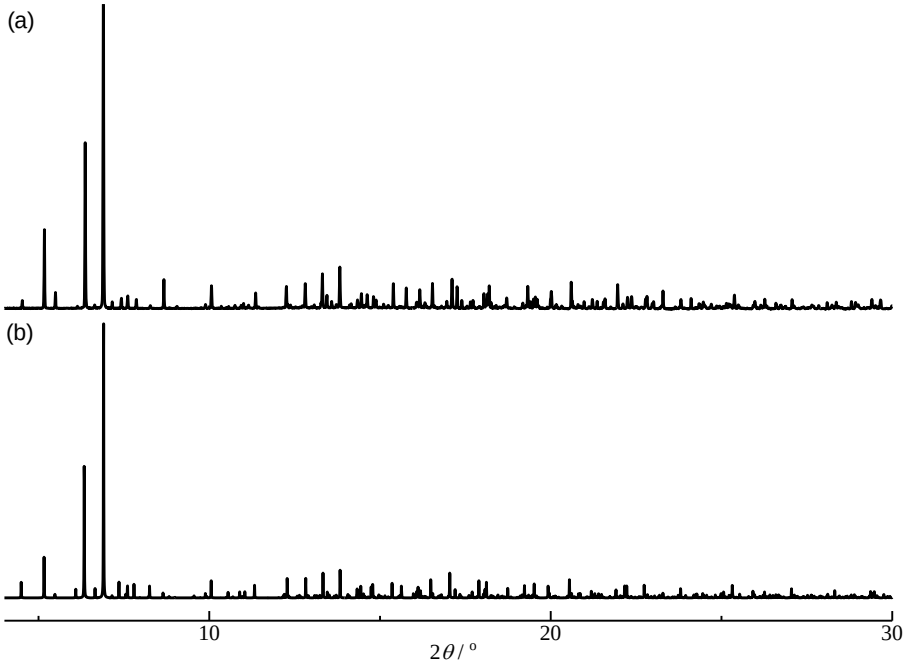

Fig. S3. (a) Experimental and (b) simulated PXRD patterns of [**2**]Br_4.

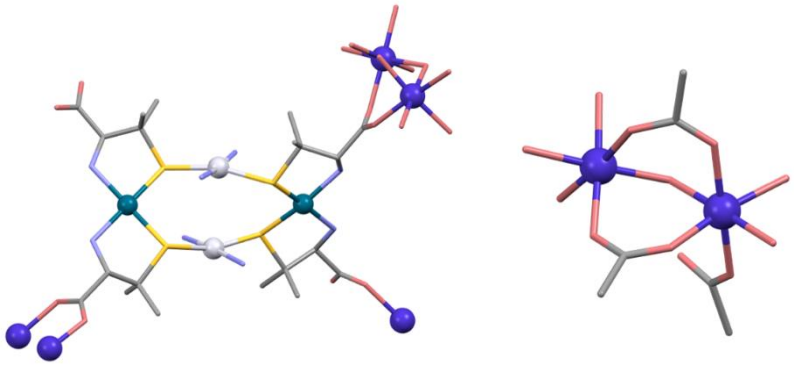

Fig. S4. Perspective views (left) around the $Pt^{II}_2Pd^{II}_2$ molecule, and (right) around the Co^{II}_2 unit in [**2**]Br_4. Hydrogen atoms are omitted for clarity. Colour code: Pd, dark green; Pt, off-white; Co, blue; S, yellow; N, light blue; O, pink; C, grey.

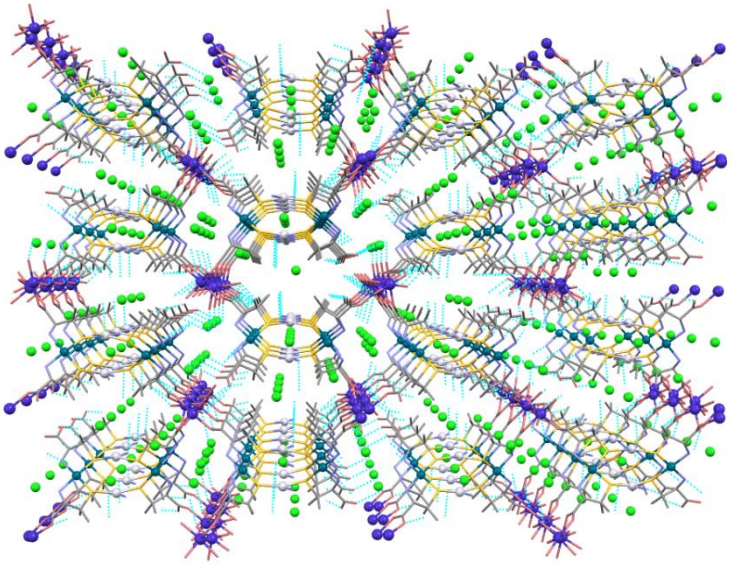

Fig. S5. Packing structure of [**2**]Cl_4. Blue dashed lines represent hydrogen bonds. Colour code: Pd, dark green; Pt, off-white; Co, blue; Cl, green; S, yellow; N, light blue; O, pink; C, grey.

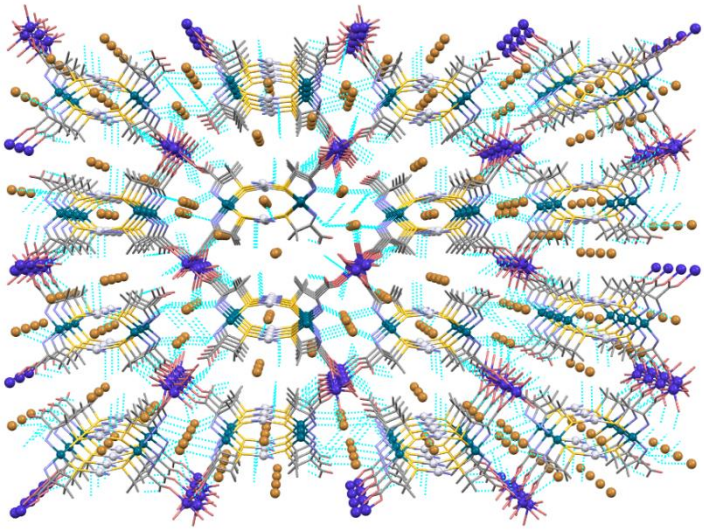

Fig. S6. (a) Packing structure of [**2**]Br_4. Blue dashed lines represent hydrogen bonds. Colour code: Pd, dark green; Pt, off-white; Co, blue; Br, brown; S, yellow; N, light blue; O, pink; C, grey.

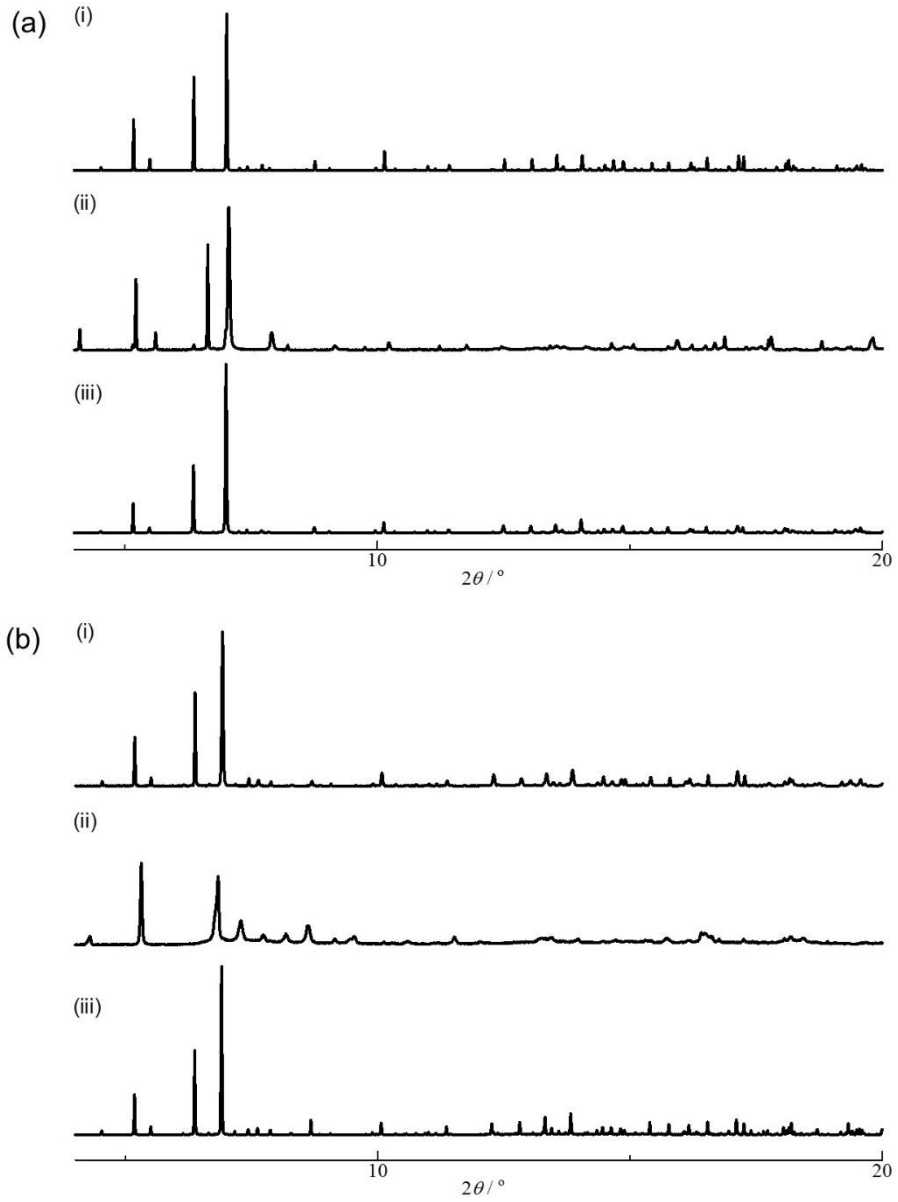

Fig. S7. Powder X-ray diffraction patterns of (i) [**2**]X_4, (ii) the sample ([**2'**]X_4) obtained by heating [**2**]X_4 at 90°C, and (iii) the sample obtained by exposure to [**2'**]X_4 in air: (a) X = Cl, (b) X = Br.

[**2'**]Cl_4: Calcd. for $[Co_2(H_2O)_2(\mathbf{1})]Cl_4 \cdot H_2O$: C, 15.27; H, 3.46; N, 7.12%. Anal. Found: C, 15.26; H, 3.38; N, 7.09%. [**2'**]Br_4: Calcd. for $[Co_2(H_2O)_2(\mathbf{1})]Br_4 \cdot H_2O$: C, 13.72; H, 3.11; N, 6.40%. Anal. Found: C, 13.55; H, 3.07; N, 6.28%

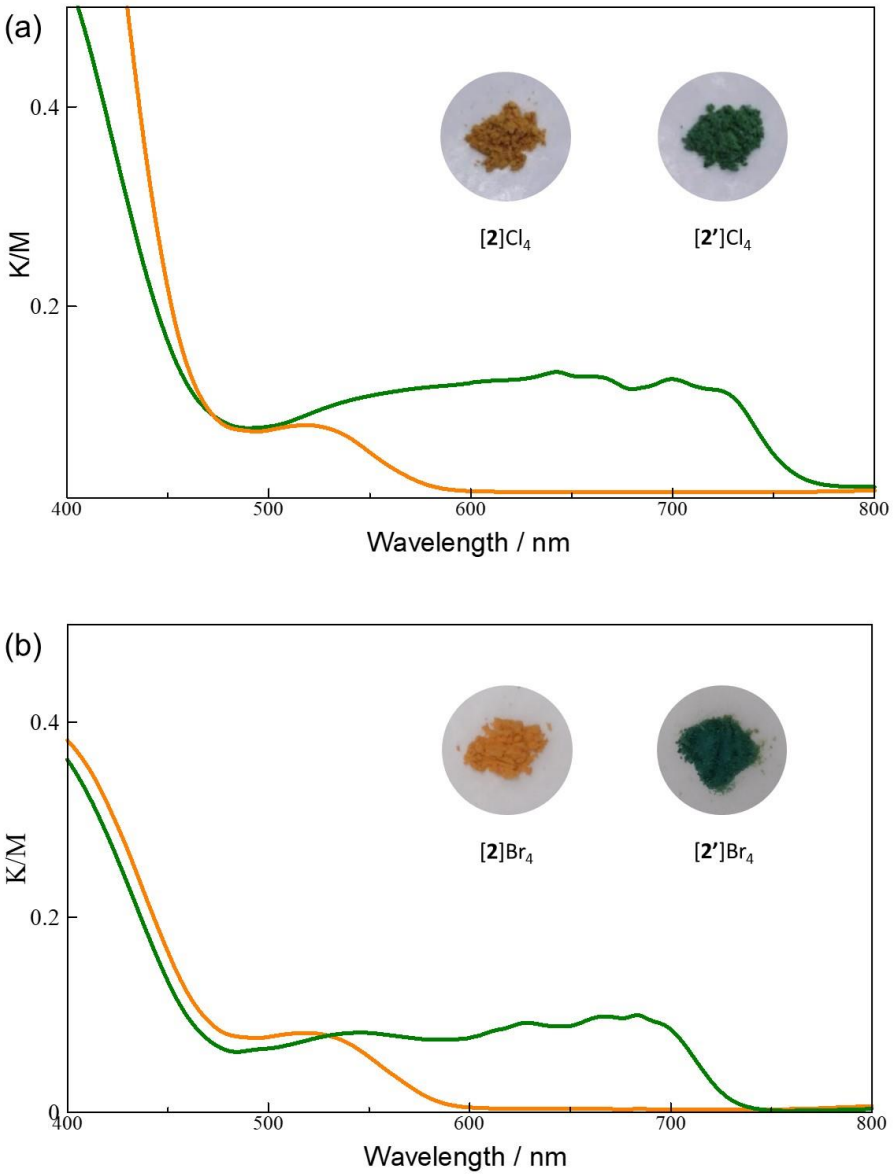

Fig. S8. Diffuse reflectance spectra of [**2**]X_4 (orange) and [**2'**]X_4 (green): (a) X = Cl, (b) X = Br.

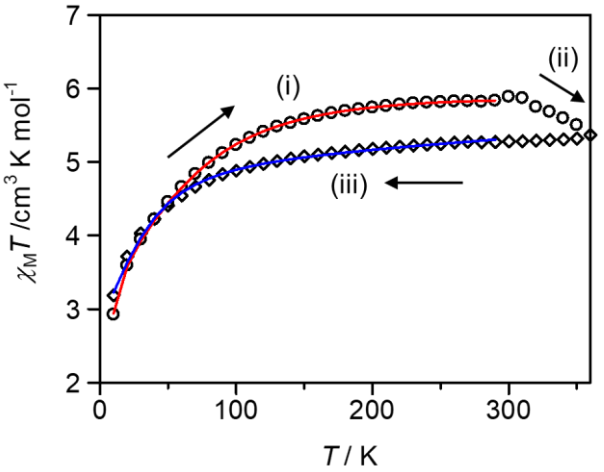

Fig. S9. $\chi_M T$ *vs.* T plot of [**2**]Br_4 (T = 10–360 K, and H = 0.5 T). Black circles and diamonds indicate the observed data. Red and blue lines indicate the fitting curves. The measurements with increasing temperature from 10 K to 300 K showed an anomaly at approximately 300–360 K, which corresponds to the transformation from [**2**]Br_4 to [**2'**]Br_4.

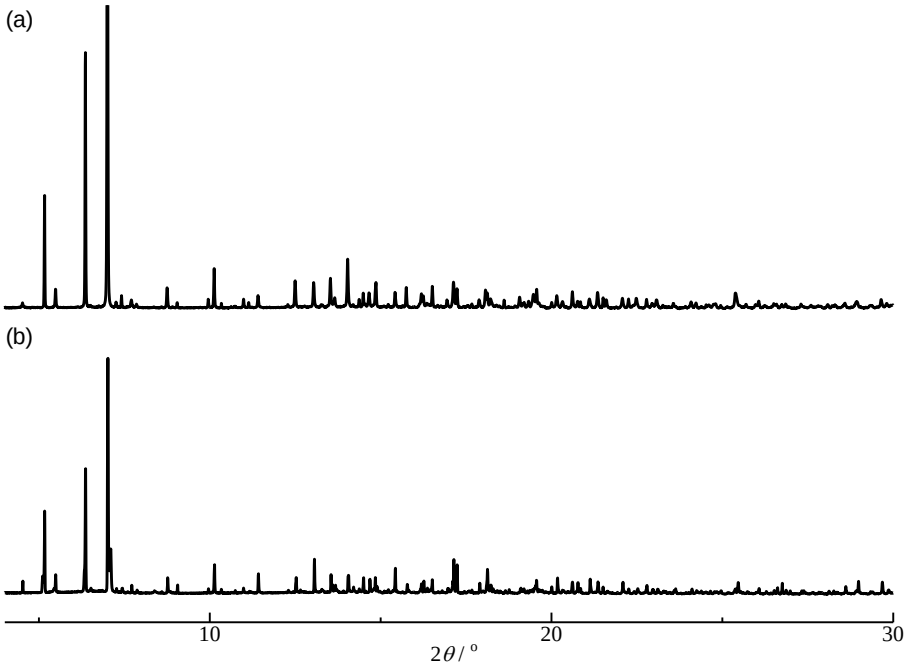

Fig. S10. PXRD patterns of [**2**]Cl_4 (a) before and (b) after bulk electrolysis at -1.2 V.

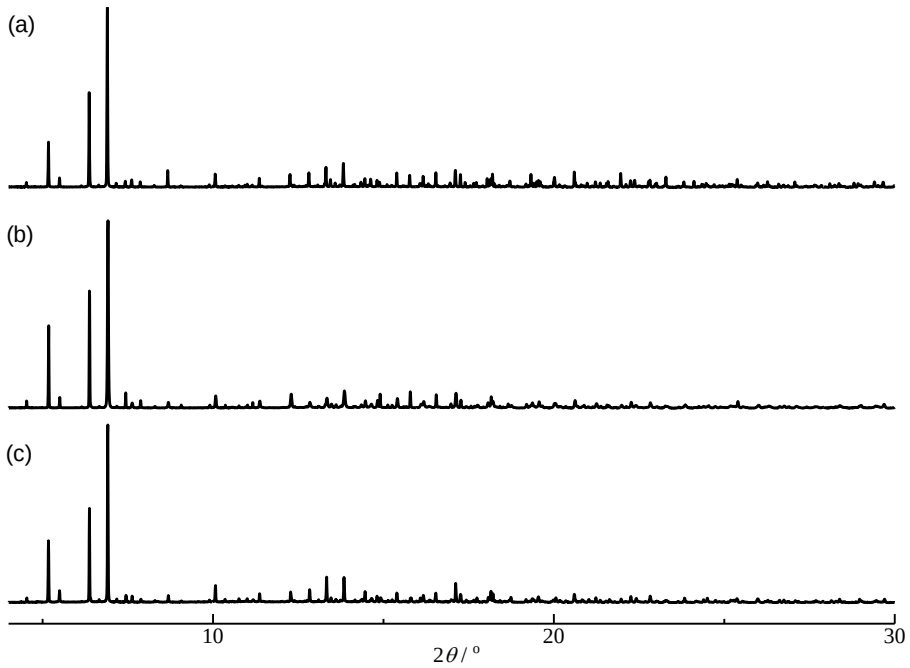

Fig. S11. PXRD patterns of [**2**]Br_4 (a) before and after (b) -1.2 V and (c) +1.2 V bulk electrolyses.

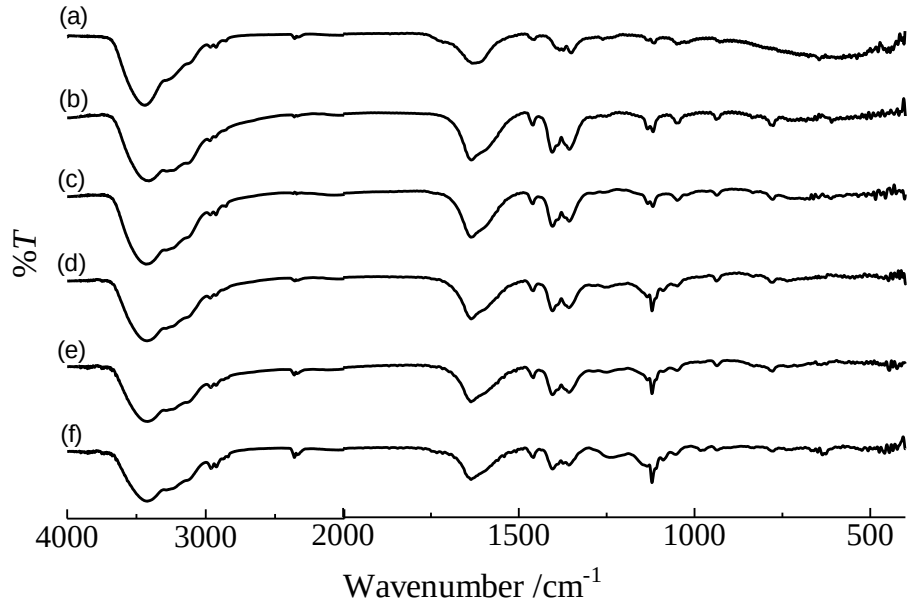

Fig. S12. IR spectra of original samples of (a) [**1**], (b) [**2**]Cl_4, and (c) [**2**]Br_4 and after bulk electrolysis at -1.2 V of (d) [**2**]Cl_4, (e) [**2**]Br_4 and at +1.2 V of (f) [**2**]Br_4.

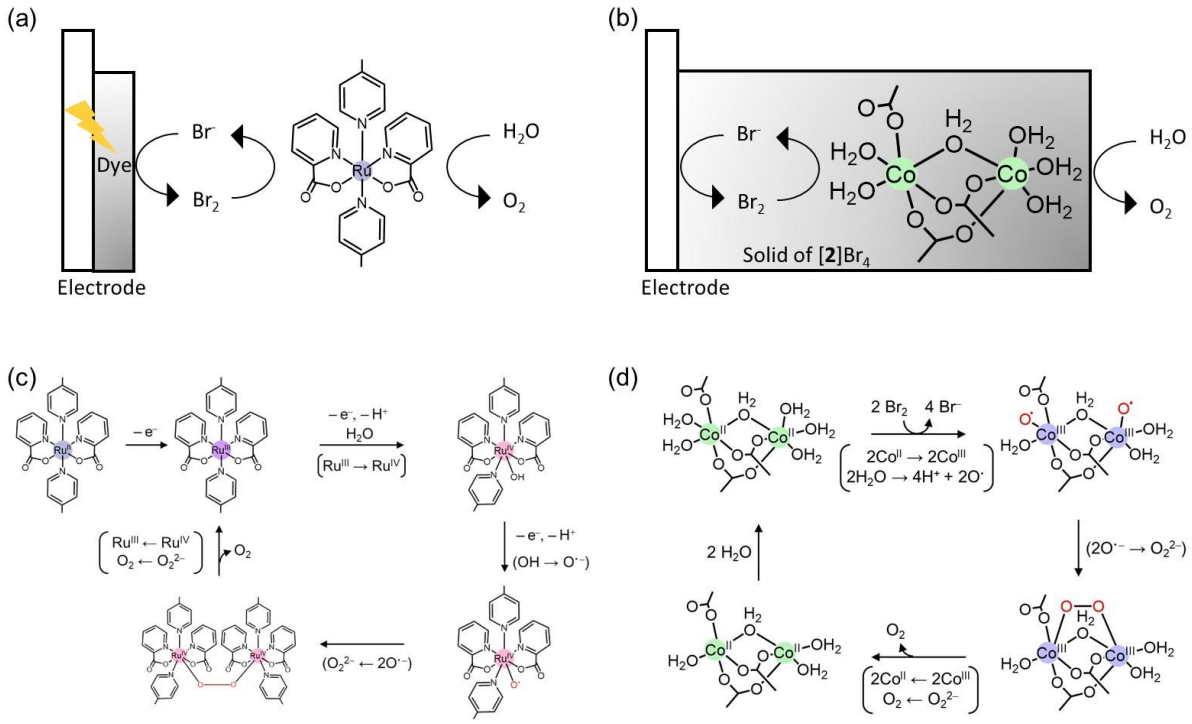

Fig. S13. Proposed mechanisms of (a, c) light-driven water oxidation catalysed by [Ru(bda)(pic)$_2$] (bda = 2,2'-bipyridine-6,6'-dicarboxylate, pic = picoline) [S6] and (b, d) electrocatalytic water oxidation catalysed by [**2**]Br$_4$.

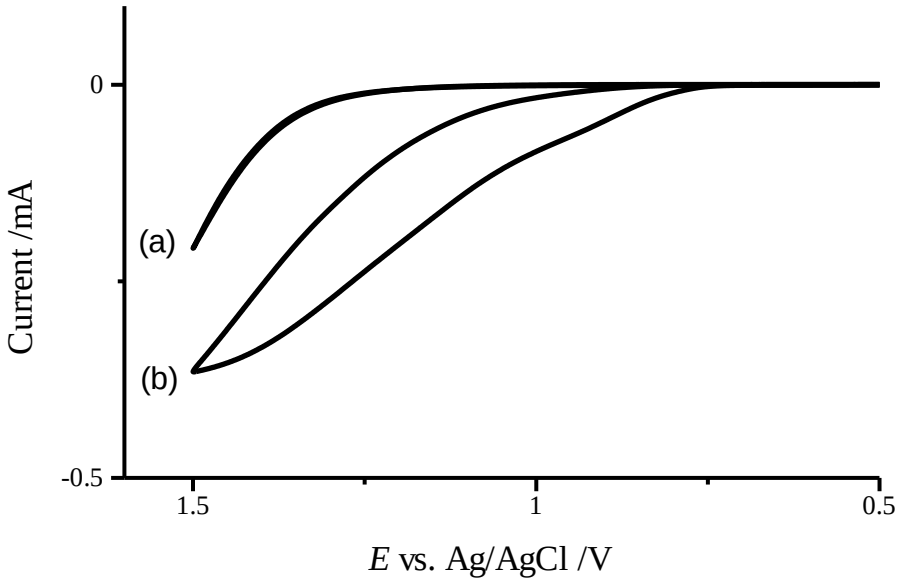

Fig. S14. CVs of (a) [**2**]Cl_4 and (b) [**2**]Br_4 in H_2O-CH_3CN (v/v =1/4) containing 0.1 M $LiClO_4$ at a scan rate of 10 mV s^{-1}.

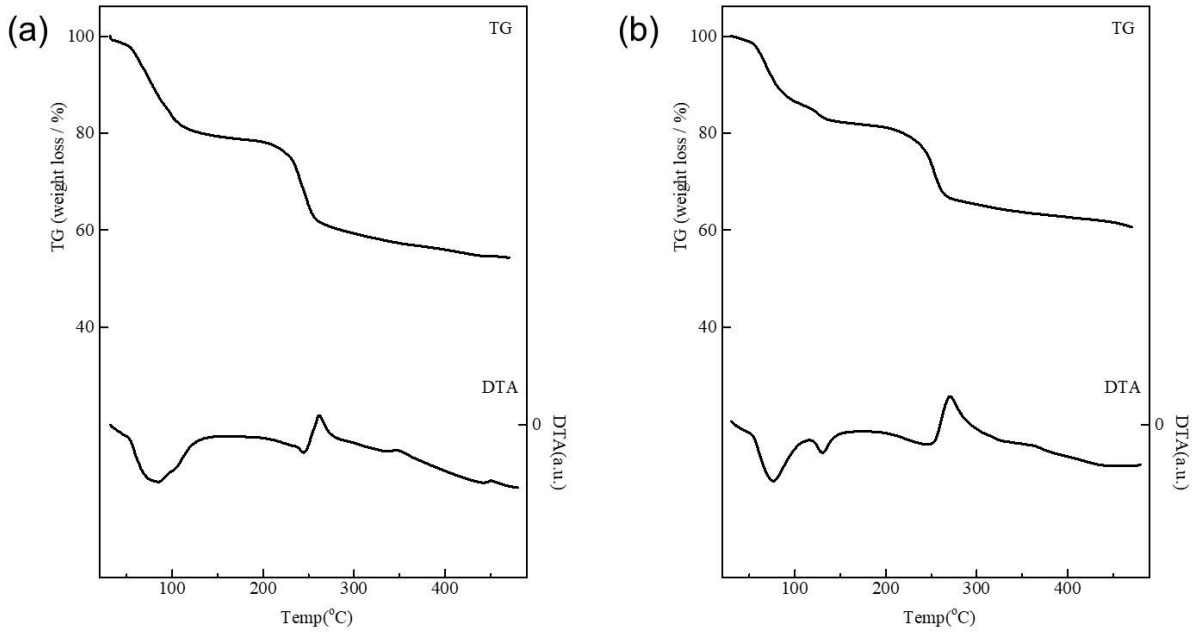

Fig. S15. TG-DTA curves of (a) [**2**]Cl_4 and (b) [**2**]Br_4.

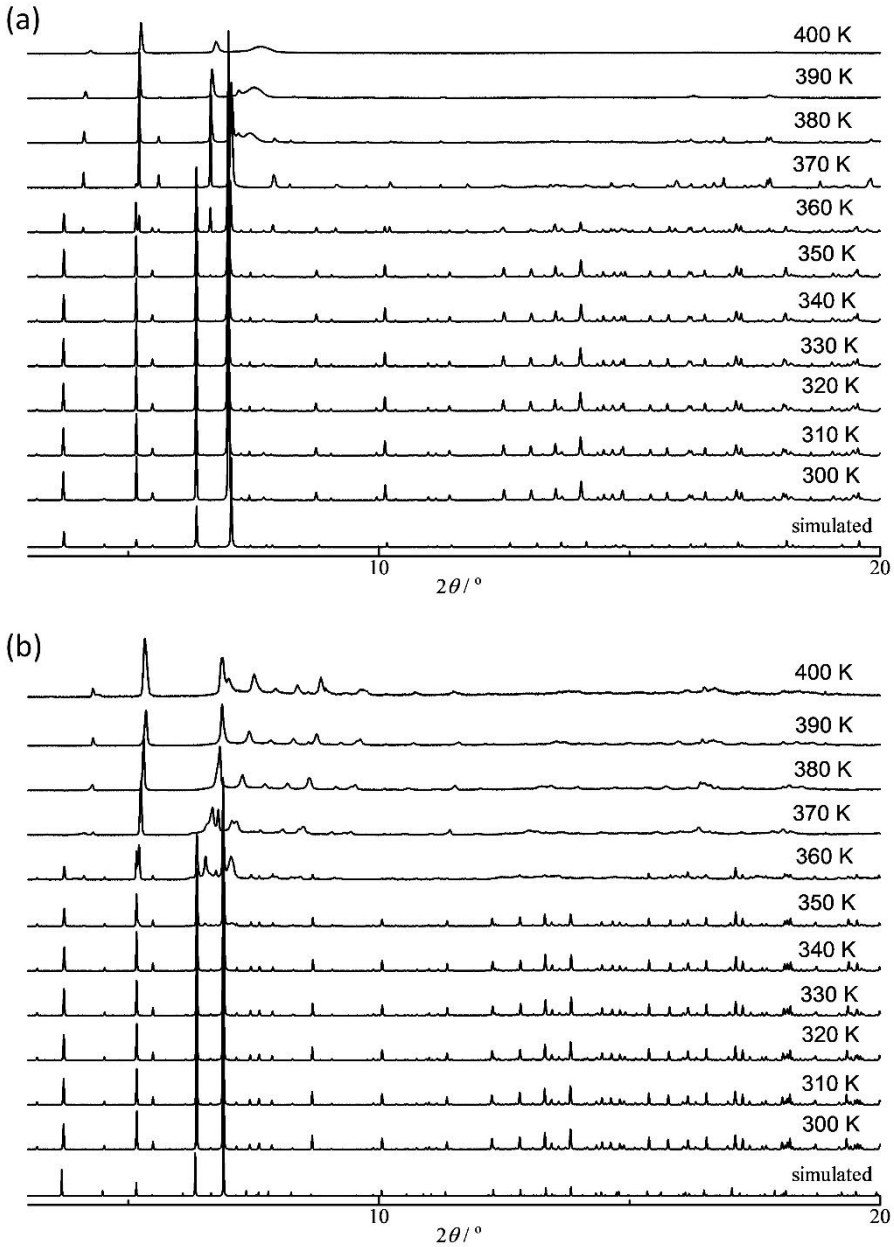

Fig. S16. Temperature-dependent PXRD patterns of (a) [**2**]Cl_4 and (b) [**2**]Br_4.

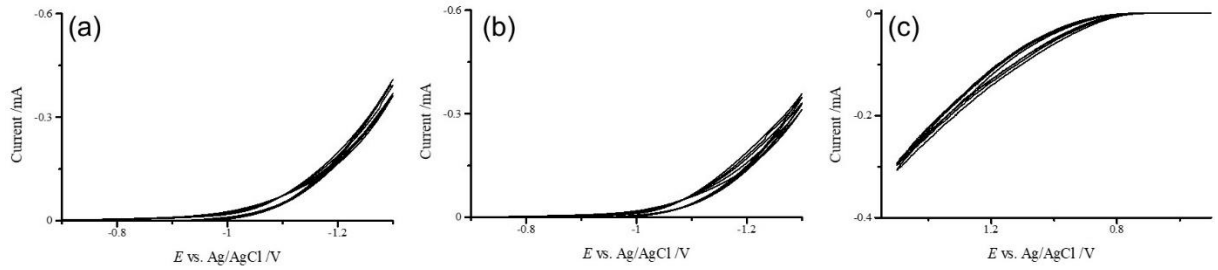

Fig. S17. Cyclic voltammograms of the samples modified on glassy carbon electrode in H_2O-CH_3CN (v/v = 1/4) containing 0.1 M $LiClO_4$ in the multi-scanning mode (1st – 5th scans): (a) [**2**]Cl_4 in the negative potential range, (b) [**2**]Br_4 in the negative potential range and (c) [**2**]Br_4 in the positive potential range.

References.

[S1] R. M. Wood and G. J. Palenik, *Inorg. Chem.* 1998, **37**, 4149.

[S2] A. C. M. San Esteban, N. Kuwamura, T. Kojima and T. Konno, *Inorg. Chem.* 2020, **59**, 14847.

[S3] N. Kuwamura, Y. Kurioka, N. Yoshinari and T. Konno, *Chem. Commun.* 2018, **54**, 10766.

[S4] Y. Gong, H. F. Shi, Z. Hao, J. L. Sun and J. H. Lin, *Dalton Trans.* 2013, **42**, 12252.

[S5] P. Manna, S. Debgupta, S. Bose and S. K. Das, *Angew. Chem. Int. Ed.* 2016, **55**, 2425.

[S6] M. V. Sheridan, Y. Wang, D. Wang, L. Troian-Gautier, C. J. Dares, B. D. Sherman and T. J. Meyer, *Angew. Chem. Int. Ed.* 2018, **57**, 3449.